Nacelle lidar for power curve measurement - Avedøre campaign

Wagner, Rozenn; Davoust, Samuel

Publication date:
2013

Document Version
Publisher's PDF, also known as Version of record

Nacelle lidar for power curve measurement _ Avedøre campaign

DTU Vindenergi
Report 2013

Rozenn Wagner, Samuel Davoust

DTU Wind Energy E-0016

January 2013

DTU Vindenergi
Institut for Vindenergi

Forfatter(e): Rozenn Wagner, Samuel Davoust
Titel: Avedøre campaign
Institut: DTU Wind Energy

Resume (maks. 2000 char.):

Wind turbine power performance requires the measurement of the free wind speed at hub height upstream of the turbine. For modern multi-megawatt wind turbines, this means that the wind speed needs to be measured at great heights, from 80m to 150m. The standard wind speed measurement with a cup anemometer, requiring the erection of a tall met mast, then becomes more and more challenging and expensive. A forward looking lidar, mounted on the turbine nacelle, combines the advantages of a nacelle based instrument - no mast/platform installation difficulties - and those of the lidar technology - remote measurement of the wind speed away from the instrument.

In the first phase of the EUDP project: “Nacelle lidar for power performance measurement”, a measurement campaign with a nacelle lidar prototype placed on an onshore turbine demonstrated the potential of the technology for power curve measurement. The main deviations of this method to the requirement of the IEC 61400-12-1 were identified and a procedure was established for the use of a nacelle lidar specifically for power curve measurement. This report describes the results of a second measurement campaign aiming at testing and finalising the procedure.

January 2013

Projektnr.:
EUDP: Nacelle lidar for power performance measurement (journal no. 64009-0273)

Sider: 36
ISBN: 978-87-92896-22-3

Technical University of Denmark
Department of Wind Energy
Brovej
Building 118
DK-2800 Kgs. Lyngby
Denmark

www.vindenergi.dtu.dk

Preface

This report describes the results from a measurement campaign carried out with a Wind Iris nacelle-mounted lidar in the Avedøre wind farm. This measurement campaign was the third phase of the EUDP project: “Nacelle lidar for power performance measurement”, after a first measurement campaign at Høvsøre test site for large wind turbines and the definition of a procedure to measure a power curve with a nacelle-based lidar. The third and last phase aimed at testing and finalising the procedure.

Content

Resume

Wind turbine power performance requires the measurement of the free wind speed at hub height upstream of the turbine. For modern multi-megawatt wind turbines, this means that the wind speed needs to be measured at great heights, from 80m to 150m. The standard wind speed measurement with a cup anemometer, requiring the erection of a tall met mast, then becomes more and more challenging and expensive. A forward looking lidar, mounted on the turbine nacelle, combines the advantages of a nacelle based instrument - no mast/platform installation difficulties - and those of the lidar technology - remote measurement of the wind speed away from the instrument.

In the first phase of the EUDP project: “Nacelle lidar for power performance measurement”, a measurement campaign with a nacelle lidar prototype placed on an onshore turbine demonstrated the potential of the technology for power curve measurement. The main deviations of this method to the requirement of the IEC 61400-12-1 were identified and a procedure was established for the use of a nacelle lidar specifically for power curve measurement. This report described the results of a second measurement campaign aiming at testing and finalising the procedure.

1. Introduction

In the first phase of the project, a measurement campaign with a nacelle lidar prototype placed on an onshore turbine demonstrated the potential of the technology for power curve measurement [1]. The main deviations of this method to the requirement of the IEC 61400-12-1 [2] were identified and described in [3]. It showed the necessity for calibrating the lidar prior to the power curve measurement. The way to calibrate the lidar was extensively investigated and two methods were developed [4]. Furthermore, a procedure was also established for the use of a nacelle lidar specifically for power curve measurement [5]. Finally a second measurement campaign was carried out with a Wind Iris series product placed on an offshore turbine in order to test and finalise the procedure. This report describes the results of this measurement campaign. The report follows the steps of the procedure [5].

2. Experimental setup

2.1 Avedøre wind farm

This report describes measurements carried out with a Wind Iris nacelle mounted Lidar on a Siemens multi-megawatt turbine belonging to the Avedøre wind farm in the period from the 22-05-2012 to the 29-10-2012. The Avedøre wind farm is located at the coast line of Avedøre Holme which is approximately 10 km south-west from central Copenhagen. The location of the wind farm is shown in Figure 1. The nacelle lidar was installed on the wind turbine labeled “T3” in Figure 1.

Two other turbines (“T1” and “T2”) are located on the west side of T3 at approximately 450m and 800m. On the north east of T3 is the Avedøre power station with tall and large buildings (dimensions?).

There was a met mast (“M”) at 2 rotor diameters (2D) to the south west (210°) of T3. It is a lattice mast instrumented with a top-mounted Thies cup anemometer at hub height and a boom-mounted wind vane 4 m below hub height according to the IEC 61400-12-1 [2]. Two boom-mounted cup anemometers, 2m below hub height and at lower tip height were used to evaluate the vertical shear.

The top cup anemometer was broken on the 30-08-2012; it was replaced by a new cup anemometer (of the same make) on the 21-09-2012. For the analysis presented in this report, the data obtained with both cup anemometers were used together (full period of measurement with the lidar). The comparison of the new cup anemometer to the lidar results in a slightly larger deviation, 0.5%, than that obtained with the old cup, 0.2% (see Appendix A). This very small difference may be due to the different wind speed distributions and different conditions (different seasons). The two cup anemometers were considered as identical.

Figure 1 Avedore Google Earth picture. The nacelle lidar is on turbine T3 and the met mast is denoted M. (T3 : 340504E 6164663N WGS84/ETRS89 Zone 33; M: 340384E 6164455N WGS84/ETRS89 Zone 33)

2.2 Nacelle Lidar setup

2.2.1 Measurements

The nacelle lidar used in this measurement campaign was a Wind Iris from Avent Lidar Technology. It is a pulsed system with 2 lines of sight separated by horizontal angle of 30° (half angle α=15°). The lidar emits a stream of pulses along each line of sight, switching between the two alternatively. This provides consecutive measurements of two radial speeds (projection of the wind speed along the line-of-sight) along each direction, at several distances simultaneously. In the following, the 10 minute average radial wind speeds are noted $<V_0>$ (for the left-hand line of sight when looking forward from behind the lidar optical head) and $<V_1>$ (for the right-hand line of sight). The 10 minute average horizontal wind speed and direction are retrieved from the averaged radial wind speeds, based on the assumption that the wind speed is horizontally homogeneous. Average longitudinal and transversal wind speed components V_x and V_y are first computed as:

$$\langle V_x \rangle = \frac{\langle V_0 \rangle + \langle V_1 \rangle}{2 \cos \alpha} \quad (1)$$

$$\langle V_y \rangle = \frac{\langle V_0 \rangle - \langle V_1 \rangle}{2 \sin \alpha} \quad (2)$$

The average horizontal wind speed <V> is then retrieved by computing the vector modulus:

$$\langle V \rangle = \sqrt{\langle V_x \rangle^2 + \langle V_y \rangle^2} \quad (3)$$

Also, the average horizontal wind direction (relative to the lidar axis) is obtained by:

$$Dir_{Lidar} = atan2(\langle V_y \rangle; \langle V_x \rangle) \quad (4)$$

The nacelle lidar was calibrated prior to being mounted on the turbine. The inclinometers calibration revealed an offset of 0.4° in the tilt/pitch angle. The offset could have been implemented in the lidar software, but it was chosen to leave it as such for more transparency. The offset was accounted for (manually) during the lidar installation and when the tilt measurements were used in the analysis.

The wind speed measurement was calibrated with the “Line of sight calibration method” and showed a very good comparison to the reference sonic anemometer. Therefore, no correction was applied to the lidar wind speed given by the lidar in this measurement campaign. The calibration method and the uncertainty results are described in details in [4].

2.2.2 Mounting and data acquisition

The lidar optical head was installed on the roof of the nacelle 5 m behind the rotor plane and 1.8 m above the turbine hub. It was tilted downward by 0.7° in order to account for the height of the optical head above hub height and for the backward tilting of the nacelle when the turbine is operating. This pre-inclination angle was calculated (according to equation (5)) so that the laser beams reached hub height at 2.5D for the wind speed giving the maximum power coefficient. The drawing in Figure 2 summarizes the setup.

$$\begin{aligned} \beta_{pretilt} &= Arctan\left(\frac{1.8}{2.5D + 5}\right) - 0.32° - 0.08° + \beta_{tilt_{corr}} \\ &= -0.7° + \beta_{tilt\_corr} \end{aligned} \quad (5)$$

H is the height of the lidar beams over hub height.
D is the turbine rotor diameter, $\beta_{Ope\_tilt} = 0.32°$ is the operational tilt from the turbine at maximum Cp, $\beta_{sta\_tilt} = 0.08°$ is the static tilt during the installation assuming the turbine nacelle is facing the wind, $\beta_{tilt\_corr} = 0.4°$ is the tilt correction to contrasts tilt error found in the calibration (thus with opposite sign of the error),

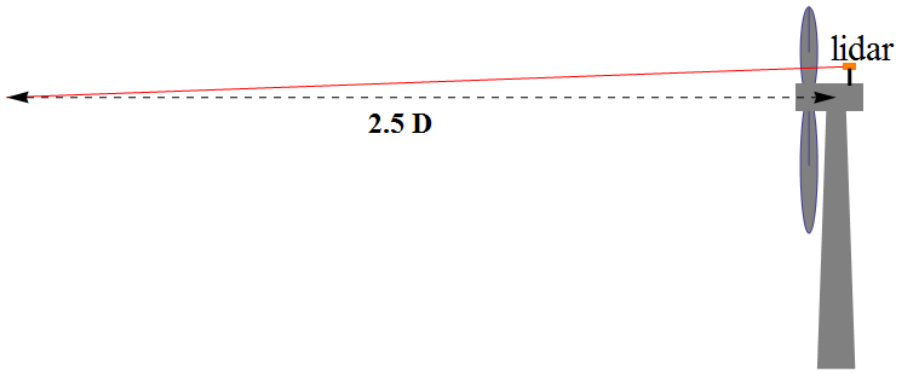

Figure 2: Overview of the measurement setup

The lidar was configured to measure at 10 ranges from 220m to 400m, including 2D and 2.5D (where D is the turbine rotor diameter) in front of the turbine. The sampling rate was set to 1.4Hz. The effective probe length is 60m.

The lidar was synchronized to all other measurements through an NTP server. High frequency 1.4Hz data and 10 min statistics were acquired and downloaded periodically from the lidar MySQL data-base. Meteorological and wind turbine data were acquired by the Siemens Wind Power data acquisition system. This system was also regularly synchronised to an NTP server. Data from both systems were combined in a DTU database in such a way that the 10 minute lidar and wind turbine data were synchronised.

3. Data selection

3.1 Turbine status

According to the IEC 61400-12-1, the data for which the turbine indicated a “failure” status were excluded.

3.2 Wind sector

3.2.1 Wind sector theoretically determined with the formula

The sector to be excluded shall be centred on the direction from the neighbouring obstacle (or wind turbine) to the wind turbine under test. As long as the total beam opening angle of the lidar is smaller than 30 degrees, the width of the sector is given by:

$$\alpha L = 1.3 Arctan\left(2.5\ \frac{Dn}{Ln-Lb} + 0.15\right) + 10 \quad (6)$$

where D_n is the rotor diameter of the neighbouring turbine, L_n the distance to the neighbouring turbine and Lb is the lidar measurement range.

Therefore, the sector 48°-112°must be excluded because of the buildings of the power station and the sector 230°-321° because of the turbine T2. The usable sectors for the power curve measurement with the lidar are 321° – 48° and 112° – 230°. However, in order to be able to make a comparison with the measurements from the met mast, only the offshore sector (112°-230°) was used.

In the case where no mast is available, the screening could be based on the turbine yaw, assuming it was calibrated prior to the beginning of the measurements. However, this would assume that the turbine is perfectly aligned with the wind direction, which is not always the case. The lidar on the other hand measures the wind direction relative to its axis. If the lidar axis is perfectly aligned with the turbine nacelle axis, this corresponds to the turbine yaw misalignment. Therefore the actual wind direction can be obtained by adding the relative measurement from the lidar to the turbine yaw.

3.2.2 Selecting the data from the usable sector based on wind direction obtained from the turbine yaw and the relative direction from lidar

The turbine used in this measurement campaign was correctly aligned with the wind direction on average as shown in Figure 3.

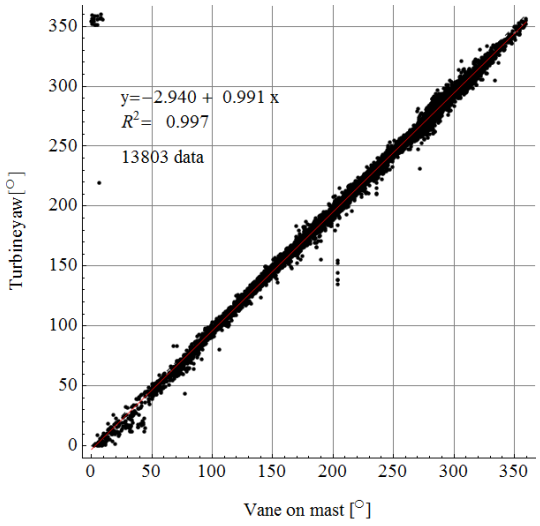

Figure 3 Comparison and linear regression between the turbine yaw and the direction indicated by the wind vane on the met mast

However, a major issue when using a nacelle lidar to obtain the wind direction is that the lidar cannot make the difference between a misalignment between the wind direction and its axis (turbine yaw error for example) and a situation where the wind speed is not horizontally homogeneous. For instance, if one of the lidar beam is in the wake of a surrounding obstacle, whereas the second beam is outside the wake (large inhomogeneity in the wind speed seen by the two beams), the lidar gives a large relative wind direction angle even though the lidar is well aligned with the wind direction. Selecting the data within the sector defined above using the wind direction obtained by summing up the lidar relative wind direction and the turbine yaw can result in selecting data outside the right sector, as shown in Figure 4. Figure 5 shows the variation of the difference between the wind speed measure by the lidar and the cup anemometer with the turbine yaw. When both beams are outside the wakes of the neighboring obstacles, the wind speed given by the lidar is very close to that given by the cup anemometer. On the other hand, when one of the beams is in a wake, the lidar gives wrong wind speeds.

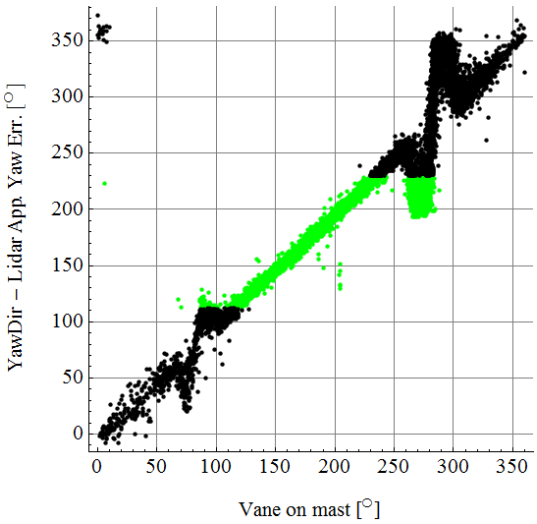

Figure 4 Comparison between the wind direction obtained by subtracting the lidar relative direction to the turbine yaw and the direction given by the vane on the met mast. The lidar relative direction is subtracted and not added because the sign convention of the lidar is positive when it increases clockwise. Each dot is a 10 min average value. The green dots are the data for which the combination of the yaw and the lidar relative angle is within 112°-230° and the black dots the data for which it is outside 112°-230°.

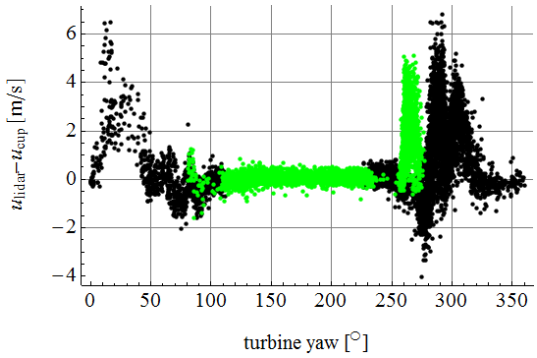

Figure 5 Difference between lidar speed and cup anemometer speed vs turbine yaw. The green dots are the data for which the combination of the yaw and the lidar relative angle is within 112°-230° and the black dots the data for which it is outside 112°-230°.

Therefore, selecting the data simply based on this parameter would result in a dataset including data that should be rejected (see green dots in Figure 4). It is necessary to apply a complementary filtering based on the variation of the relative wind direction given by the lidar and/or on the comparison of the turbulence intensity along the two lines-of-sight, i.e. the ratio between the standard deviation and the average value of the radial speed.

3.2.3 Complementary filtering based relative wind direction as a function of yaw

Figure 5 shows that the lidar relative wind direction is close to 0° on average only for turbine yaw values between 110° and 250°. Therefore the data with a yaw outside this range should be rejected. Figure 6 shows the corresponding wind speed difference between the lidar and the cup anemometer measurement.

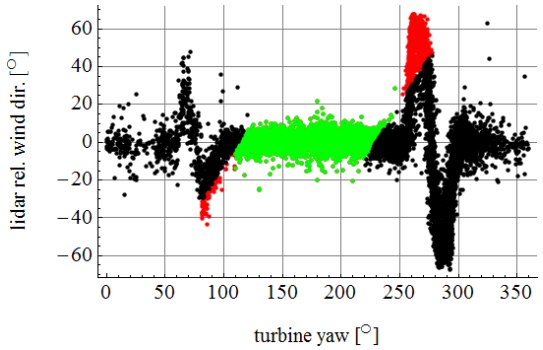

Figure 6 Relative wind direction given by the lidar vs turbine yaw. Black dots: data rejected by first filtering (selection for wind direction within 112° and 230° based on the combination of the turbine yaw and the lidar relative wind direction); Red: rejected by the second filtering (based on the turbine yaw), green dots: data selected for power curve

3.2.4 Complementary filtering based on the difference between the turbulence intensity along the two lines of sight as a function of yaw

A similar analysis can be done by looking at the difference between the turbulence intensity along the two lines of sight. Indeed, while both lidar beams measure in a homogeneous wind, the turbulence intensity along the two lines of sight are expected to be very similar, whereas, in an inhomogeneous wind (like when one beam is inside and the other outside the wake of an obstacle), they are expected to be significantly different, as shown in Figure 7. The turbulence intensity is very similar along the two line-of-sights for yaw values between 110° and 250°, the sector selected in the previous section.

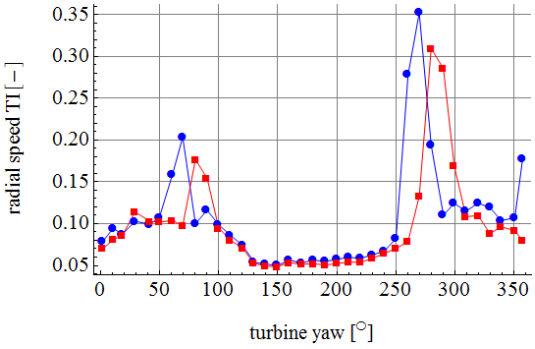

Figure 7 Radial speed turbulence intensity along the two line-of-sight (beam 0 in blue and beam 1 in red) vs turbine yaw.

3.3 Lidar availability

The “RWS availability” is an output parameter of the Wind Iris. It is the ratio between the number of valid radial wind speed measurements and the total number of expected horizontal wind speed measurements (=number of streams of pulses) in ten minutes. The number of streams of pulses emitted in 10 minutes is almost constant (varying between 852 and 853). Therefore the RWS availability corresponds to the relative number of valid measurements in 10 minutes. It is given for each line of sight separately (RWS0 and RWS1). The availability of the lidar measurements can be affected by the blade passage in front of the lidar (preventing the laser beam to propagate beyond the rotor) and by the aerosol distribution in the air in front of the turbine.

Most of the data have a RWS availability above 0.75 (see Figure 8 and 10). The availability does not have a significant influence on the lidar deviation (i.e. difference between the lidar horizontal wind speed and the cup anemometer horizontal wind speed), except for very low availability (below 0.4), see Figure 11. To ensure the quality and quantity of data used in this investigation, it was chosen to select data with a RWS availability above 0.75.

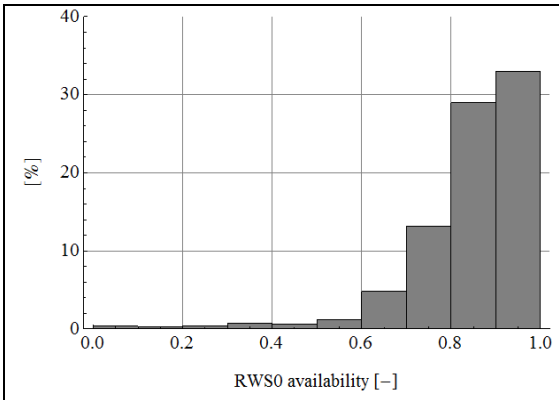

Figure 8 Distribution of the 10 min availability of the radial wind speed measured by the lidar alonf the first line of sight(RWS0 availability)

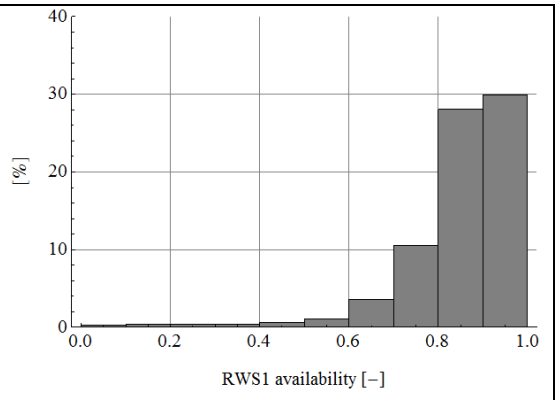

Figure 9 Distribution of the 10 min availability of the radial wind speed measured by the lidar alonf the first line of sight(RWS0 availability)

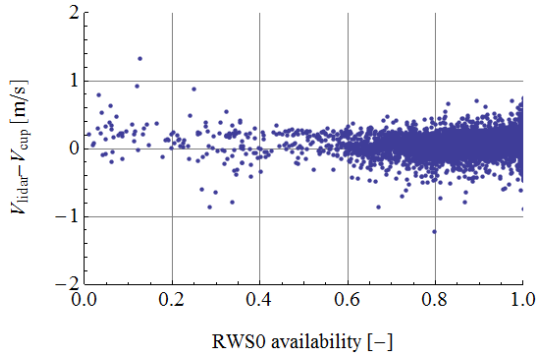

Figure 10 Difference between the lidar wind speed and the cup anemometer wind speed at 2D vs the lidar’s RWS0 availability

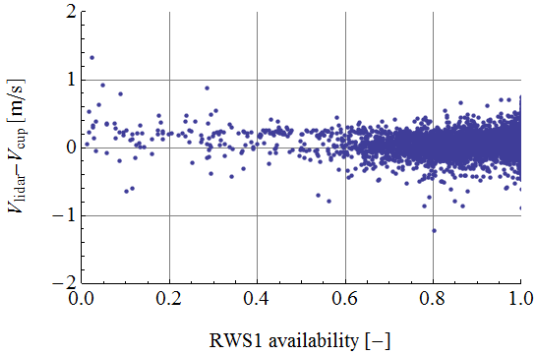

Figure 11 Difference between the lidar wind speed and the cup anemometer wind speed at 2D vs the lidar’s RWS1 availability

The 10 min lidar data availability increases with the turbine rotor speed (see Figure 12 and 14), therefore with the wind speed (see Figure 14 and 16). As the blades pass faster in front of the lidar beam, a larger number of pulses can get through in between the blades. As shown in Figure 14 and 16, from a certain rotor speed (0.7 x rated speed), the blades pass fast enough to ensure a valid measurement for every stream of pulses and therefore get an availability of 1. Discarding data with availability lower than 0.75 does not remove low wind speed data and therefore does not affect the power curve measurement.

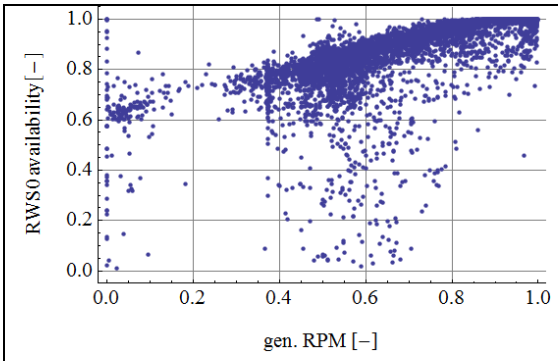

Figure 12 Radial speed availability along first beam vs generator RPM.

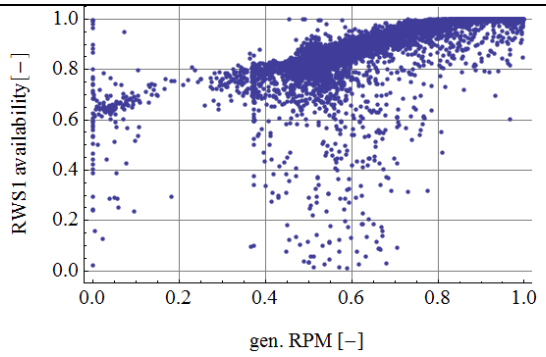

Figure 13 Radial speed availability along second beam vs generator RPM.

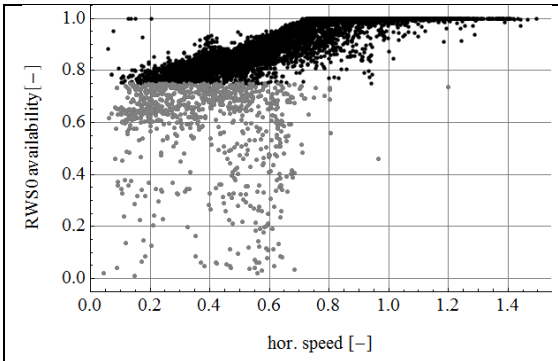

Figure 14 Lidar's RWS0 availability vs wind speed (measured by cup anemometer at hub height). Black: data with more than 0.75 availability; gray: data with less than 0.75 availability

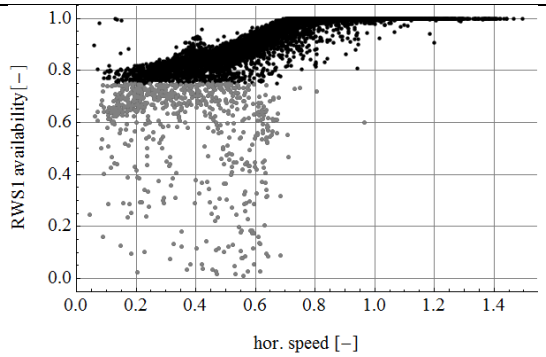

Figure 15 Lidar's RWS1 availability vs wind speed (measured by cup anemometer at hub height). Black: data with more than 0.75 availability; gray: data with less than 0.75 availability

It can be seen from Figure 14 and 16, that the RWS availability below 0.75 does not depend on the wind speed. These low values are probably due to reasons other than the blade passage. The low availability is related to a low CNR (i.e. CNR<-22dB) as shown in Figure 16 and 18. The CNR was low for both lines of sight, but it was not exactly identical. As shown in Figure 18, this low CNR mainly occurred in the 6 first days of the measurement campaign and in the middle of August. Figure 19 shows that the CNR was similar for all measurement ranges.

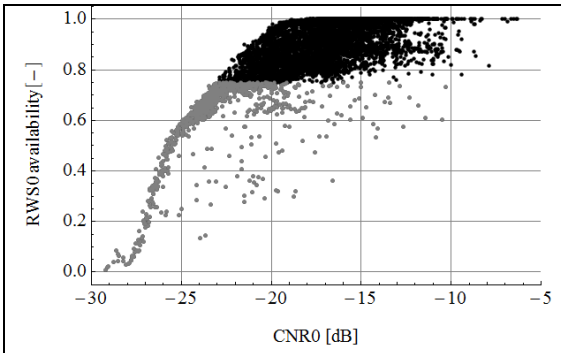

Figure 16 RWS0 availability vs CNR0 (CNR of first beam). Data with an availability higher than 0.75 (black), data with an availability lower than 0.75 (gray).

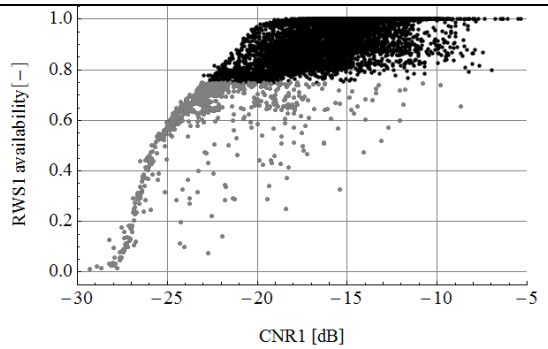

Figure 17 RWS1 availability vs CNR1. Data with an availability higher than 0.75 (black), data with an availability lower than 0.75 (gray).

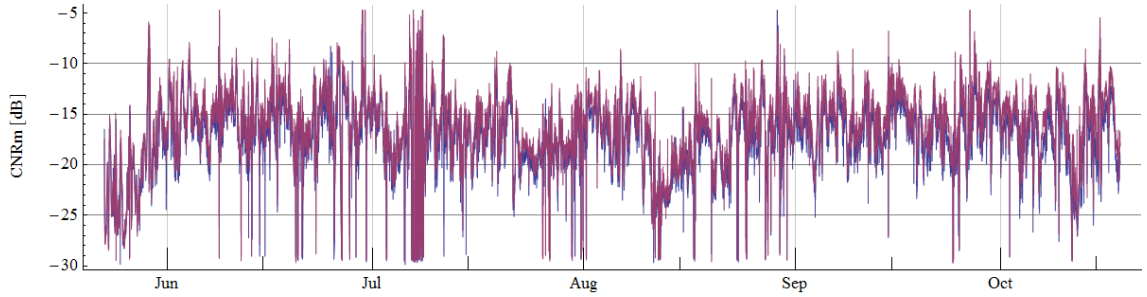

Figure 18 Time series of the 10 min mean CNR of beam 0 (blue) and beam 1 (red)

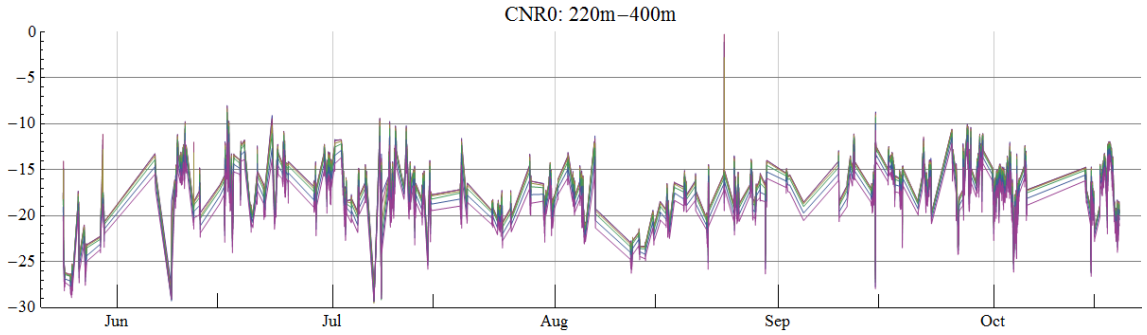

Figure 19 Time series of the 10 min mean CNR of beam 0 at the different ranges between 220m and 400m (only for filtered data)

Note however that an availability of 0.75 only ensures that every 10 min average radial speed was calculated with a minimum of 639 valid measurements. There is no clear and direct way to know how these measurements were distributed in time within the 10 min period; and therefore there might be some large gaps in the 10 minute time series. In order to avoid large gaps due to one blade standing in front of the laser beam, the data with a generator rotation speed below 0.375 x max. RPM were discarded, as shown in Figure 20.

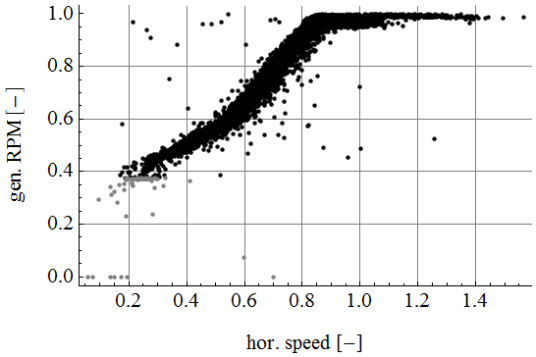

Figure 20 Generator RPM vs horizontal wind speed.

4. Tilt, roll and measurement height

4.1 Tilt and roll

Two pairs of inclinometers, installed in the lidar optical head, enabled us to control the tilt (backard-forward motion) and roll (side to side motion) of the lidar. The tilt and roll were monitored throughout the whole measurement campaign. The lidar optical head follows the turbine nacelle motions. As shown in Figure 21, the mean tilt increases with the wind speed up to rated speed and then decreases with increasing speed, as the blades pitch allowing the thrust on the rotor to decrease. The mean tilt varies between -1° and -0.04°. The tilt is negative since the lidar optical head was inclined downwards (see section 2.2.2). The roll increases with wind speed, see Figure 22. The roll was 0° at the installation of the lidar, therefore when the turbine was at stand still. The mean roll range (-0.3°,0.25°) is smaller than the tilt range.

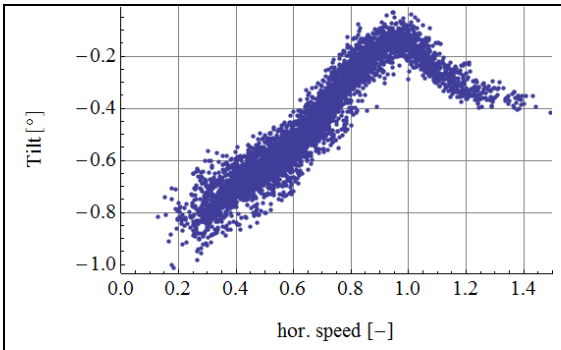

Figure 21 Lidar (10 minute mean) tilt angle vs wind speed measured by the lidar at 2D

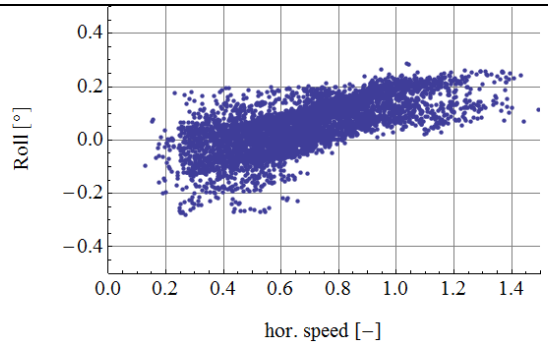

Figure 22 Lidar (10 minute mean) roll angle vs wind speed measured by the lidar at 2D

Figure 23 and Figure 24 show the 10 minute standard deviation of the tilt and roll. Figure 25 and Figure 26 show the 10 minute minimum and maximum of the tilt and roll, respectively. The tilt variations within 10 minutes increase with the wind speed but remain quite small. The roll fluctuations also increase with the wind speed and get relatively large for wind speed above 0.8 x rated speed.

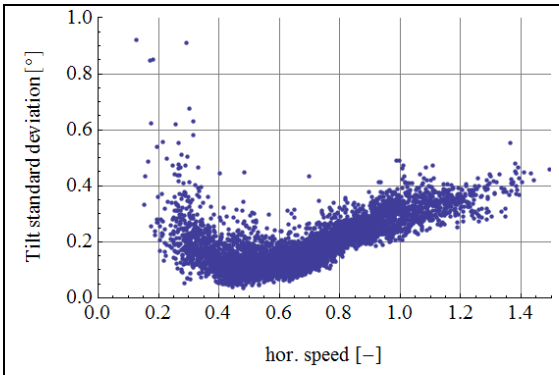

Figure 23 Standard deviation of the lidar tilt angle vs wind speed measured by the lidar at 2D

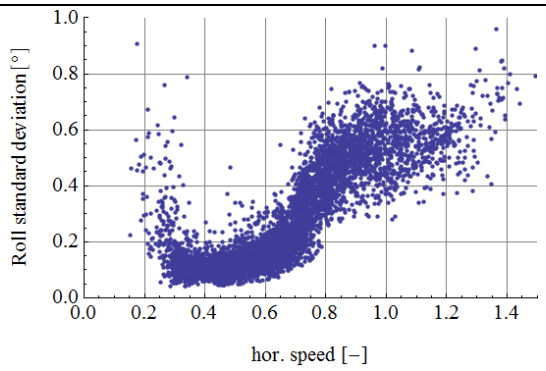

Figure 24 Standard deviation of the roll tilt angle vs wind speed measured by the lidar at 2D

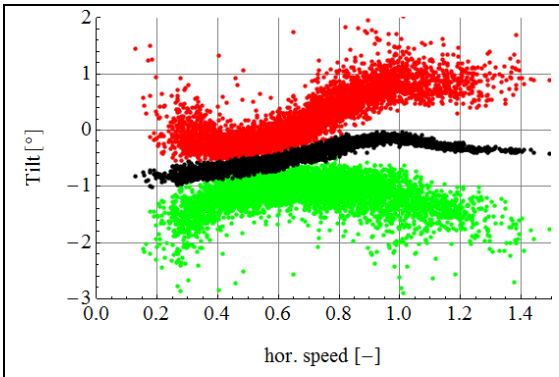

Figure 25 Tilt angle vs wind speed measured by the lidar at 2D: 10 min mean (black), minimum (green), maximum (red)

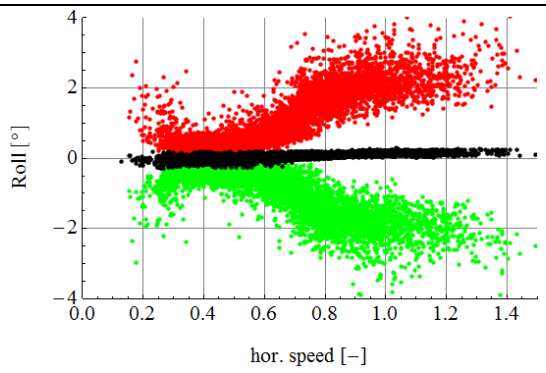

Figure 26 Roll angle vs wind speed measured by the lidar at 2D: 10 min mean (black), minimum (green), maximum (red)

4.2 Measurement height

The 10 min mean tilt angle was converted into the lidar measurement height at 2.5D in front of the rotor. As expected, the lidar was measuring at hub height for a wind speed corresponding to the maximum Cp (about 70% of rated speed). It was measuring below hub height for lower wind speeds, down to 97% of hub height for 20% of the rated speed. It was measuring above hub height for higher wind speeds, up to 101.6% of hub height for 95% of the rated power.

The measurement height falls outside the range required by the IEC 61400-12-1, for low wind speeds, see Figure 27. (For information the measurement height corresponding to the 10 minute minimum tilt and the maximum tilt are shown in appendix B.)

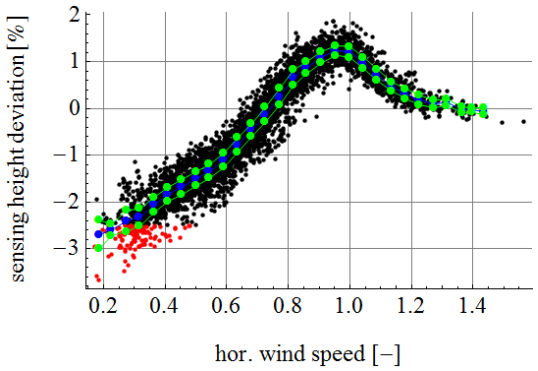

Figure 27 Lidar measurement height at 2.5D relative to hub height. 10 minute data within hub height +/- 2.5% (black),10 minute data outside the range hub height +/- 2.5% (red), averaged measurement height deviation per wind speed bin (blue), average +/- half of the standard deviation of the measurement height deviation per wind speed bin (green).

We investigated two ways to account for the fact that the measurements were taken outside the range allowed by the IEC standard: hub height +/- 2.5% of hub height. The first way was to discard the data measured outside the allowed range. However, the lidar measurement height variations depend on the flexibility of the turbine tower. If the amplitude of the nacelle tilting was larger, it could result in measuring too low for low wind speeds and too high for wind speeds around rated speed. Discarding these data would result in truncating the power curve. For the dataset used in the present analysis it is not problematic as it only removes a few data in the wind speed bins. As shown in Figure 28, the bin averaged power curves obtained with and without discarding the data are identical. It only makes a small difference in the type A uncertainty, see Figure 29.

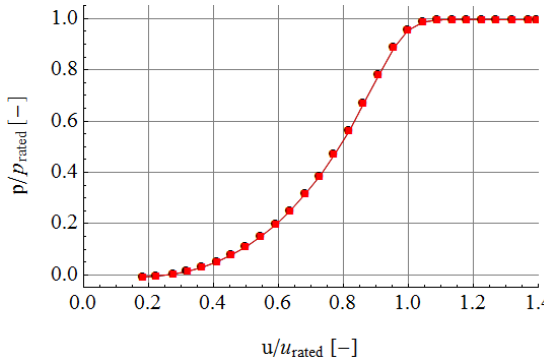

Figure 28 Bin-averaged power curves obtained with all data (black), after filtering the 10 minute data measured below 97.5% of hub height (red).

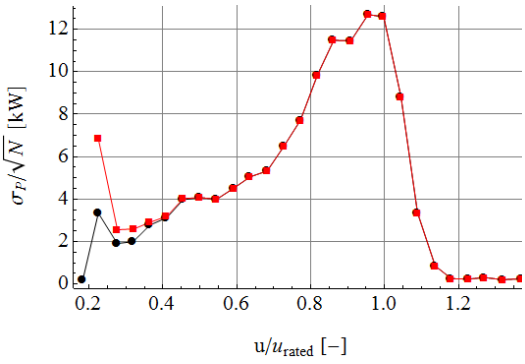

Figure 29 Category A uncertainty in power obtained with all data (black), after filtering the 10 minute data measured below 97.5% of hub height (red).

Another possibility is to keep all the data in order not to alter the power curve, but to add an uncertainty to the wind speed bins for which the average +/- the half of the standard deviation of the measurement height is outside the range. This uncertainty is quantified as the error in wind

speed due to the difference between the actual measurement height and 97.5% of hub height, assuming a power law profile with a shear exponent of 0.2:

$$u_{v3,i} = \frac{(u_{i,m} - u_{i,b})/u_{i,b}}{\sqrt{3}} \tag{7}$$

where $u_{i,m}$ is the averaged measured wind speed and $u_{i,b}$ the wind speed extrapolated to the closest range boundary: 97.5% of hub height.

$$u_{i,b} = u_{i,m}\left(\frac{0.975\, z_{hub}}{z_{i,m}}\right)^{0.2} \tag{8}$$

Where $z_{i,m}$ is the averaged measurement height and z_{hub} is hub height.

Figure 30 shows the uncertainty due to the fact that the wind speed was measured outside the range hub height +/- 2.5%, according to equation (3). According to the criteria of the bin average +/- half of the standard deviation of the measurement height deviation, for the present dataset, the extra uncertainty needs to be applied to only 4 bins. The resulting uncertainty is very small.

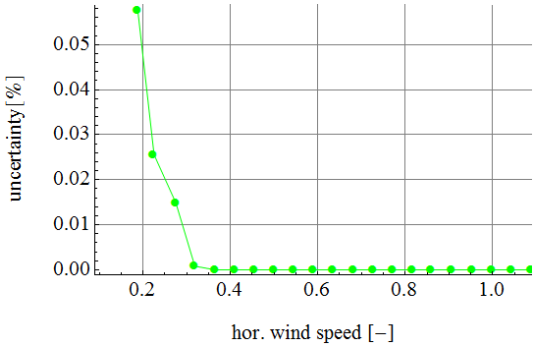

Figure 30 Relative uncertainty in wind speed due to the lidar height measurement relative to hub height vs wind speed. The uncertainty is 0% if the bin average measurement height is within the hub height +/- 2.5%.

5. Lidar wind speed measurements compared to the cup anemometer

5.1 Mean wind speed

In Figure 35 to Figure 38, the lidar (10 minute) mean horizontal wind speed is compared to the cup anemometer 10 minute wind speed. In Figure 35 and Figure 37, the data were bin-averaged according to the cup anemometer wind speed, before doing the linear regression, so that the regression is not influenced by the wind speed distribution. The linear regression obtained for the 10 min data are displayed in Figure 36 and Figure 38 for comparison purpose.

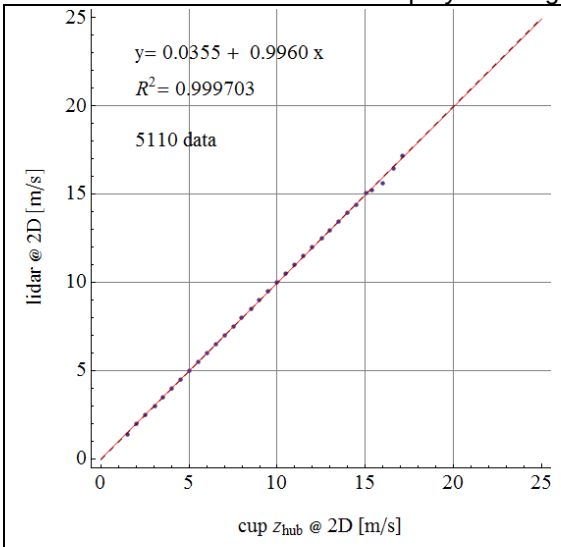

Figure 31 Linear regression between the bin-averaged wind speed measured by the lidar at 2D and the cup anemometer at 2D.

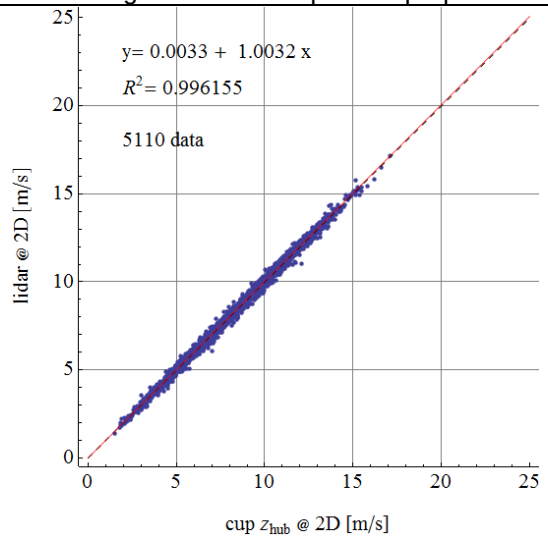

Figure 32 Linear regression between the 10 min mean wind speed measured by the lidar at 2D and the cup anemometer at 2D.

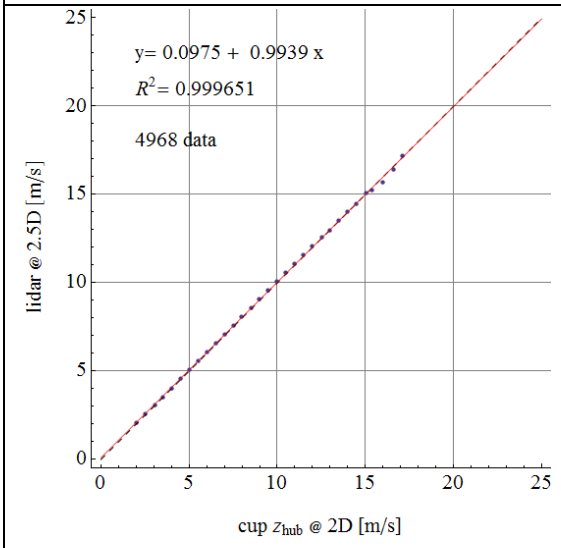

Figure 33 Linear regression between the bin-averaged wind speed measured by the lidar at 2.5D and the cup anemometer at 2D.

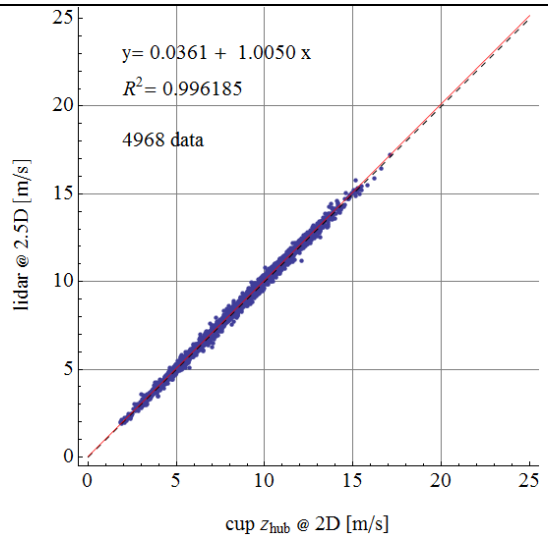

Figure 34 Linear regression between the 10 min mean wind speed measured by the lidar at 2.5D and the cup anemometer at 2D.

Table 1 Relative wind speed deviation between the lidar and the cup anemometer at 2D for a wind speed of 10m/s.

	Bin-averaged data	10 min mean data
Lidar at 2D vs cup	-0.045%	0.353%
Lidar at 2.5D vs cup	0.365%	0.861%

5.2 Power curve

In this section, the focus is on the difference obtained between the wind speed measured with the lidar and the with the cup anemometer. Therefore the same air density correction, using the mast temperature, was applied to both measurements. The two power curves are very similar, see Figure 39. The lidar power curve, measured at 2D, results in an underestimation by of the AEP smaller by 0.6% that that obtained with the cup anemometer power curve (for an average wind speed of 8 m/s).

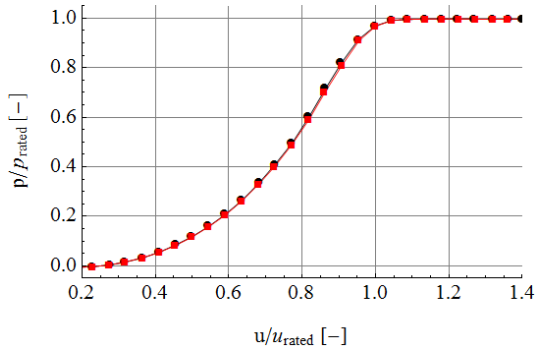

Figure 35 Bin averaged power curve: with the cup anemometer measurements (black); with the lidar measurements (red).

The scatter plots are very similar. A larger scatter appears in both power curves around 0.9-1.0 normalised wind speed, see Figure 40 and Figure 41; further investigation showed that it is related to the vertical shear. In spite of this, the category A uncertainty obtained with the nacelle lidar is slightly smaller on average than that obtained with the cup anemometer (see Figure 42).

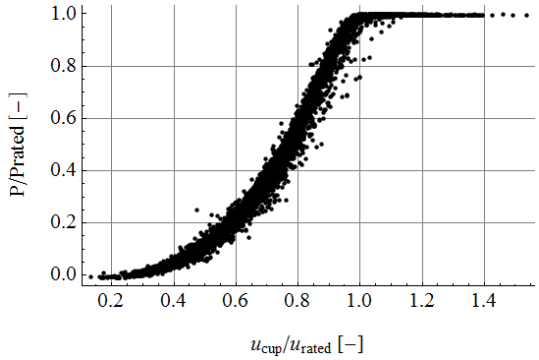

Figure 36 Power curve scatter plot obtained with the cup anemometer at hub height at 2D

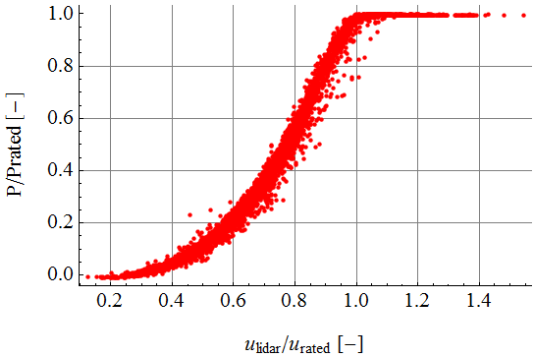

Figure 37 Power curve scatter plot obtained with the lidar at 2D

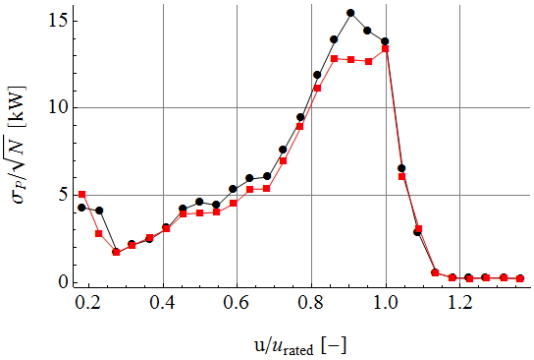

Figure 38 Category A uncertainty vs normalised wind speed for the power curve obtained with the cup anemometer (in black), with the lidar (in red).

5.3 Wind speed measurement uncertainty

The total category B uncertainty in wind speed for the lidar includes 4 sources of uncertainty:

1) The lidar calibration uncertainty ;
2) The uncertainty due to the terrain orography;
3) The uncertainty related to the measurement height (if this one goes out of the range hub height +/- 2.5%);
4) The uncertainty of the tilt inclinometers.

5.3.1 Calibration uncertainty

The lidar was calibrated for each line of sight separately. The calibration uncertainty for each line of sight includes the reference sonic anemometer uncertainties, the uncertainty for finding the precise line of sight orientation, the uncertainty of the vertical position of the beam relative to the sonic, the mean offset between the 10 minute mean wind speeds measured simultaneously by both instruments the uncertainty of this offset and the statistical uncertainty of the lidar measurements. This is explained and described in details in the calibration report [4]. The uncertainty obtained for each line of sight (beam 0 and beam 1) are displayed as a function of wind speed in Figure 43.

These uncertainties were combined geometrically in a conservative approach, assuming the uncertainty for both lines of sight were correlated with each other; based on equations (1), (2) and (3). The uncertainty of the average horizontal wind speed was calculated as:

$$u_V = \frac{\partial V}{\partial V0} u_{V0} + \frac{\partial V}{\partial V1} u_{V1} \quad (9)$$

where u_{V0} and u_{V1} are the uncertainty of the average radial speed along each line of sight. The combined uncertainty (i.e. the uncertainty of the resulting horizontal wind speed) is also shown in Figure 43 and it is in the order of magnitude as the uncertainty for each line of sight separately.

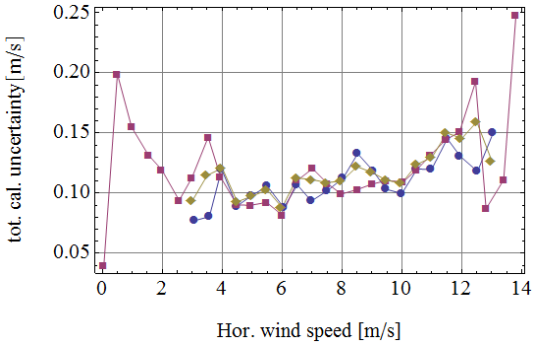

Figure 39 Blue dots: radial speed uncertainty beam 0; Purple squares: radial speed uncertainty beam 1; Yellow diamond: combined uncertainty from both beams

5.3.2 Uncertainty due to the terrain orography

The uncertainty due to the terrain orography is the same as for a power curve measured with a cup anemometer top mounted on a mast according to the IEC standard [2]. In this analysis, it was taken as 1% of the wind speed, since the measurements are taking place offshore.

5.3.3 Uncertainty due to the measurement height

The lidar beams tilt backward and forward because of the motion of the nacelle under the variations of the wind speed. For low wind speed the measurement height goes out of the rage allowed by the IEC standard: hub height +/- 2.5%. An uncertainty was added to the wind speed bins for which the average +/- the half of the standard deviation of the measurement height is outside the range. This uncertainty is quantified as the error in wind speed due to the difference between the actual measurement height and 97.5% of hub height, assuming a power law profile with a shear exponent of 0.2, according equation (7) and (8). As shown in Figure 30, the uncertainty in measurement height is below 0.045%.

5.3.4 Uncertainty of the tilt inclinometers

The uncertainty of the tilt inclinometers should be derived from the calibration. It was assumed to be u_{T1}=0.1°. To be perfectly fair, the nacelle tilting during the lidar installation, which depends on the wind speed and direction relative to the turbine nacelle, should also be taken into account. This uncertainty was assumed to be u_{T2}=0.2°.

The uncertainties of these angles were converted in an uncertainty in measurement height at the measurement range used for the power curve measurement: 2.5D:

$$\Delta H = 2.5D \ \tan(u_{T1} + u_{T2}) \tag{10}$$

Finally, it is converted to a wind speed uncertainty assuming a power law profile with a shear exponent of 0.2:

$$u_{v4} = \left(\left(\frac{z_H+\Delta z}{z_H}\right)^{0.2} - 1\right)/\sqrt{3} \tag{11}$$

where z_H is the hub height. This results in a relative uncertainty (in %). For an uncertainty of 0.1° in tilt angle, the relative uncertainty is 0.19% of the wind speed.

5.3.5 Combined category B uncertainty in wind speed

The combined category B uncertainty in wind speed was obtained by addind the 4 previous uncertainties quadratically. A coverage factor of 2 is applied to the calibration uncertainty. The combined category B uncertainty in wind speed for the lidar is displayed as a function of the horizontal wind speed (bin) in Figure 44. For comparison, the category B wind speed uncertainty for the power curve obtained with the mast cup anemometer is also shown in Figure 44.

The main components of the category uncertainty in the wind speed measured with the lidar are the lidar calibration uncertainty (between 0.96% and 2.2% of the wind speed, according to Figure 43) and the uncertainty due to the distance between the lidar measurement range and the turbine rotor (1%). However, the latter component is exactly the same for the power curve measured with the top cup anemometer. The two other components of the uncertainty are very small compares to the two first ones.
The lidar wind speed uncertainty is larger than that of the cup anemometer. However, one should note that it can hardly be smaller than the uncertainty of the cup anemometer, since the sonic anemometer was used as reference instrument in the lidar calibration and the sonic anemometer is expected to have an uncertainty similar to that of the cup anemometer.

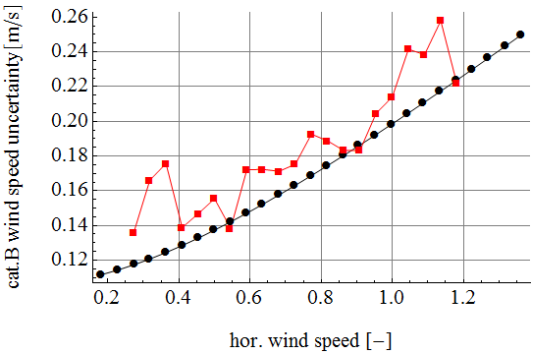

Figure 40 Combined category B uncertainty in wind speed for the power cuvre measured with the cup anemometer (black dots) and with the lidar (red squares) vs the horizontal wind speed

5.4 Total power curve uncertainty and AEP uncertainty

Category A power uncertainty and category B wind speed uncertainty were calculated for each wind sensor separately as described above. The category B uncertainties in power, temperature and pressure measurement were the same for both power curves. The total power curve uncertainty obtained with the lidar is comparable to that obtained with the cup anemometer, see Figure 45. It is on average slightly higher than the power curve uncertainty obtained with the cup anemometer. This results from the category B uncertainty in wind speed being larger for the lidar than for the cup anemometer. The negative difference in category A uncertainty in power is not large enough to compensate for the positive difference in category B uncertainty in wind speed.

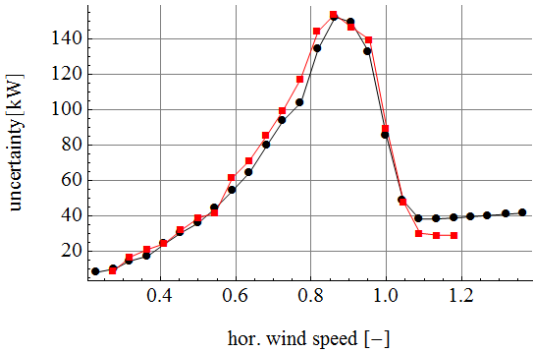

Figure 41 Total uncertainty in power curves measured with the cup anemometer (black dots); with the lidar (red squares)

Table 2 Relative AEP and uncertainty obtained with the mast cup anemometer and the nacelle lidar

	Mast top cup	Lidar
AEP for 8m/s	100%	99.4%
AEP uncertainty	3.3%	3.4%

6. Nacelle temperature for air density correction

If a power curve verification is carried out with a nacelle lidar and without any mast, it is necessary to install a sensor to measure the air temperature on the turbine. During this measurement campaign, a temperature sensor was installed on the turbine hub. The 10 minute mean temperature indicated by this sensor was compared to the air temperature measured by the sensor mounted at 2m below hub height on the met. mast. As shown in Figure 46, the nacelle sensor was underestimating the air temperature by 2°C on average, whereas an overestimation would have been more likely, because of the influence of the heating from the turbine nacelle. However, the systematic underestimation is easily explained by the fact that the sensor installed on the nacelle has not been calibrated. Therefore, the real offset of the instrument is unknown and the temperature indicated by this sensor cannot be considered as the real temperature at the turbine hub.

Nevertheless, this comparison shows a linear relation between the two sensors and thus shows that installing the temperature sensor on the turbine nacelle would be totally acceptable for power curve verification, at the condition that the sensor is calibrated prior to installation on the turbine.

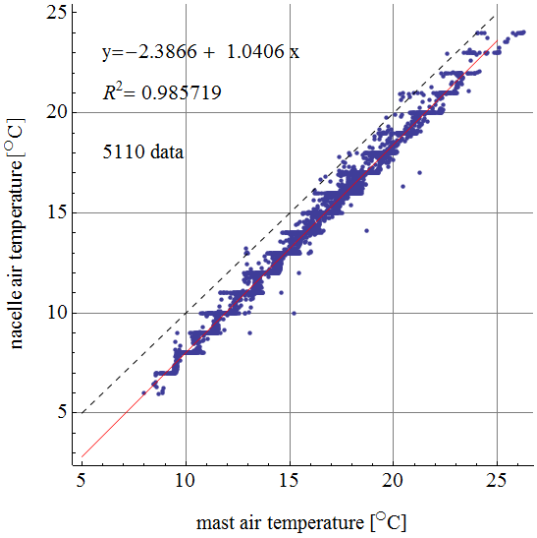

Figure 42 Air temperature measured by the sensor placed on the turbine hub vs the air temperature measured by the sensor mounted on the met mast 2m below hub height.

7. Comparison to power curve with nacelle anemometer

The most common method for power performance verification is to use an anemometer placed on the nacelle of the turbine. Therefore the nacelle lidar results have been compared to those obtained with an anemometer on the nacelle.

For the comparison, the data were selected within the limited sector 140°- 220° in order to maximize the uniformity of the flow over the nacelle. Apart from this wind sector restriction, the same filters as previously were applied: turbine status, lidar availability, minimum RPM. Thus the same dataset could be used to derive the power curve with the mast top cup anemometer, the nacelle lidar and the nacelle anemometer.

The nacelle anemometer considered in this comparison is primarily used for the turbine control and was not meant to be used for power performance verification. However, it was the only anemometer available on the nacelle measuring at the same time as the lidar. The measurements of this cup anemometer were corrected internally by the turbine manufacturer/operator. The nacelle anemometer wind speed compares very well to the mast top anemometer on average but with a very large scatter, see Figure 43. Initially, there were many outliers due to some nacelle anemometer faults. All points with ratio between the nacelle anemometer and the mast top anemometer lower that 0.875 or larger than 1.125 were excluded.

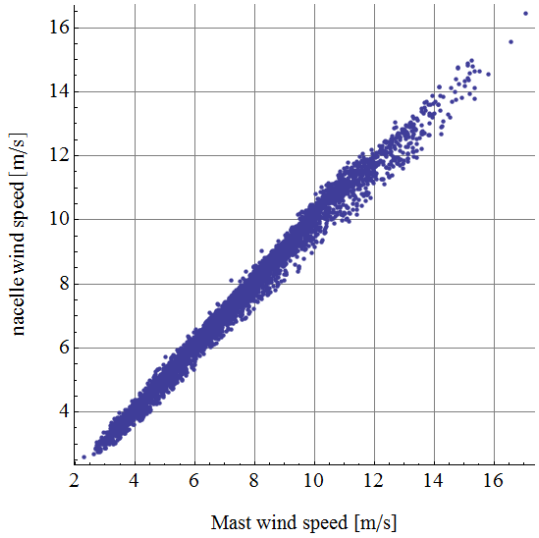

Figure 43 Comparison between the wind speed measured by the nacelle anemometer and that measured by the mast top cup anemometer.

The bin-averaged power curves obtained with all three instruments are very similar to each other, see Figure 44. The differences in AEP (for an average speed of 8 m/s) are less than 1% (see Table 2).

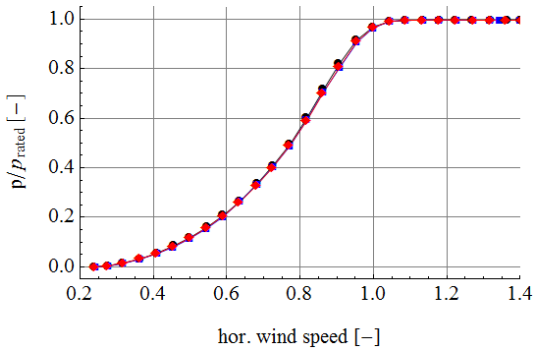

Figure 44 Bin-averaged power curves obtained with the mast top anemometer (black), the nacelle lidar (red) and the nacelle anemometer (blue). Note that the data used for the nacelle anemometer was slightly different from that used for the two other curves.

Table 3 Relative Annual Energy production for the power curve obtained with the mast top cup anemometer (reference), the nacelle lidar and the nacelle anemometer for the mean wind speed of 8m/s

	Mast top cup	Lidar	Nacelle anemometer
AEP for 8m/s	100%	99.4%	99.2%

Finally, the power statistical uncertainties obtained in the 3 curves are shown together in Figure 49. The nacelle anemometer has the largest statistical uncertainty, much larger than for the two others since there was a very large scatter in the power curve. The total uncertainty was not derived for this power curve because the comparison would not be fair since the nacelle anemometer was not meant to be used for this purpose and was not calibrated. However, the wind speed uncertainty from a nacelle anemometer is expected to be larger than that of an anemometer top mounted on a mast in front of the turbine rotor. Therefore the total power curve uncertainty is expected to be larger than that obtained with the mast and it is likely to be larger than the uncertainty obtained with the lidar.

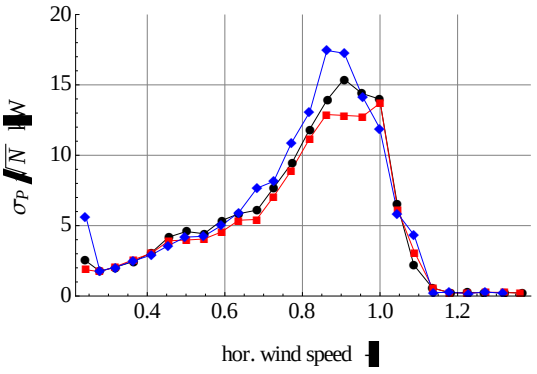

Figure 45 Category A power uncertainty for the three power curves: with the mast top cup anemometer (black), with the nacelle lidar (red) and with the nacelle cup anemometer (blue).

8. Nacelle Lidar measurement of turbulence intensity

In this section, the reference horizontal turbulence intensity measured by the cup anemometer TI_{cup} is compared to that measured by the nacelle Lidar (TI_{lidar}). With a two horizontal forward facing beam nacelle Lidar, it was observed that it was accurate and robust to use the lidar beams individually in order to retrieve turbulence intensity, by computing turbulence intensity TI_0 and TI_1 on beams 0 and 1. Turbulence intensity on each beam is defined as the standard deviation dV_i of each beam's wind speed (i=0 or 1) divided by the average beam wind speed:

$$TI_i = \frac{dV_i}{\langle V_i \rangle}$$

With:

$$dV_i = \sqrt{\langle V_i^2 \rangle - \langle V_i \rangle^2}$$

TI_{lidar} is then defined as:

$$TI_{lidar} = \frac{TI_0 + TI_1}{2}$$

Although the cup and the Lidar may not by principle measure turbulence in the exact same manner (because of important differences in spatial resolution and geometrical configuration), TI_{lidar} and TI_{cup} are found to display an encouraging level of correlation; as shows the figure below.

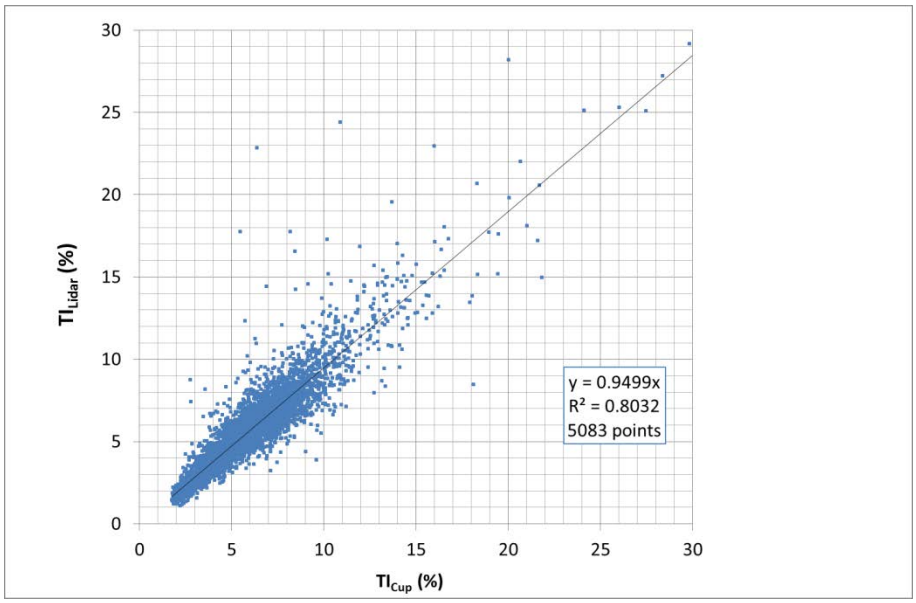

Figure 46 : Comparison between the turbulence intensity measured by the nacelle Lidar and that measured by the mast top cup anemometer (same dataset as used in section 5).

9. Conclusions

We have performed a power curve measurement with a 2-beam nacelle mounted lidar according to the procedure we have developed within the same project. The lidar was installed on an offshore multi-megawatt wind turbine close to the coast.

First, the lidar assumes to be measuring in a horizontally homogeneous wind flow. Therefore the wind sector used for the power curve must be carefully chosen, so that none of the two beams is affected by the wake of a neighbouring obstacle.

Within a horizontally homogeneous flow, the 10 minute mean wind speed measured by the lidar compared very well to the measurements of the cup anemometer mounted on a mast in front of the turbine. Consequently, the bin-averaged power curve obtained with the lidar was very similar to that obtained with the IEC standard set up, resulting in a difference in AEP of only 0.6%.

The main challenge in using this technology for power curve measurement is that the lidar tilt back and forth due to the motion of the turbine nacelle. In this campaign, most of the data were within the range recommended by the IEC standard: hub height plus or minus 2.5%. Only few points were outside this range, for low wind speeds.

Two ways of handling this issue were investigated: removing the data outside the allowed range is the most sensible method but can be problematic for turbines with more flexible towers; keeping all the data but adding an uncertainty assure to have as many data as possible in all the wind speed bins and therefore avoid truncating the power curve. However, to be totally fair, the data should probably be normalised to the closer range boundary (97.5% or 102.5% of hub height) or maybe to hub height.

In any case, this demonstrates that special care must be taken when installing the lidar on the nacelle to tilt the device in order to assure that most of (if not all) the data come from the range hub height +/- 2.5%.

The power curve statistical uncertainty is slightly smaller with the nacelle lidar than with the cup anemometer mounted on a mast in front of the turbine because the lidar always measures the incoming wind speed. Therefore the correlation between the free wind speed and the turbine power is higher with the lidar than with the cup anemometer. On the other hand, the category B uncertainties in wind speed in larger for the lidar than for the cup anemometer. This is inherent to the lidar calibration method which is based on the comparison of the lidar to a cup anemometer. The resulting combined power curve uncertainty obtained with the lidar is slightly larger than that obtained with the cup anemometer. The AEP uncertainties obtained with the two instruments were only different by 0.1%.

This analysis demonstrated that the nacelle mounted lidar is a promising technology for power curve verification if it is handled with care to the deviations from the standard approach. The main deviations are well covered by the procedure developed in this project. The main uncertainty sources have been identified but some more investigation is needed to establish the best way to evaluate them.

References

1. Wagner R et al., Nacelle lidar for power curve measurement, submitted to Wind Energy in September 2012.
2. IEC standard for wind turbine power performance measurement 61400-12-1, Edition 1 (2005)
3. Wagner R et al., Nacelle lidar power performance measurement in the context of the IEC 61400-12-1 standard, EWEA Offshore conference (2011)
4. Courtney M. (2012): Calibration of two-beam nacelle lidar, DTU Wind Energy E-0020 (2013)
5. Wagner R et al., Procedure for power curve measurement with a nacelle lidar, DTU Wind Energy E-0019 (2013)

Appendix A

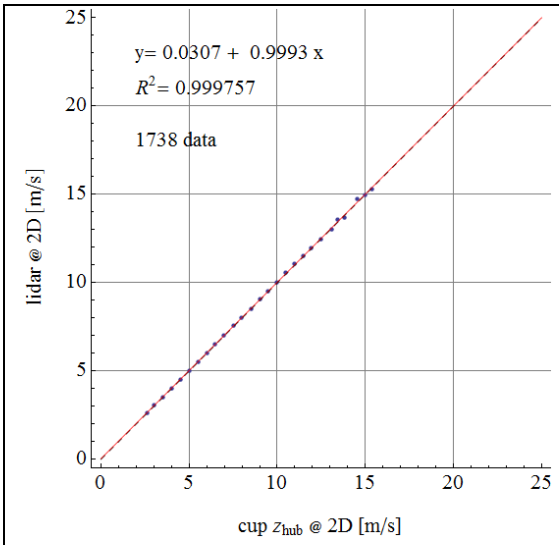

Figure 47 Comparison between the lidar and the cup anemometer (at 2D) before the 30-08-2012

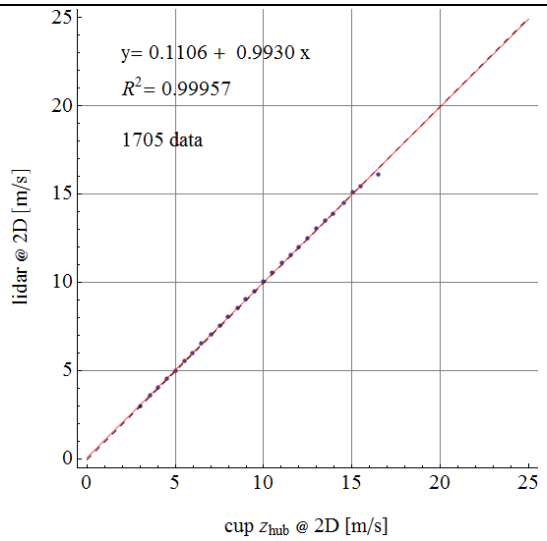

Figure 48 Comparison between the lidar and the cup anemometer (at 2D) after the 21-09-2012

Appendix B

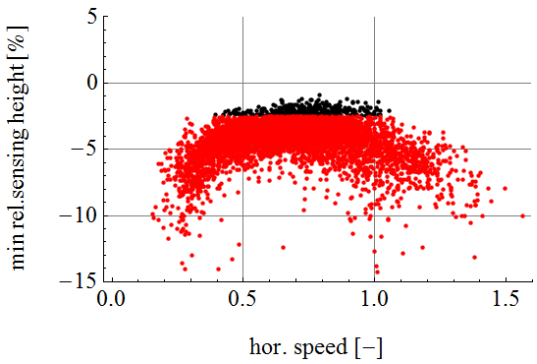

Figure 49 Measurement height (relative to hub height) corresponding to the 10 minute minimum lidar tilt; data within hub height +/- 2.5% (black), data outside the range hub height +/- 2.5% (red)

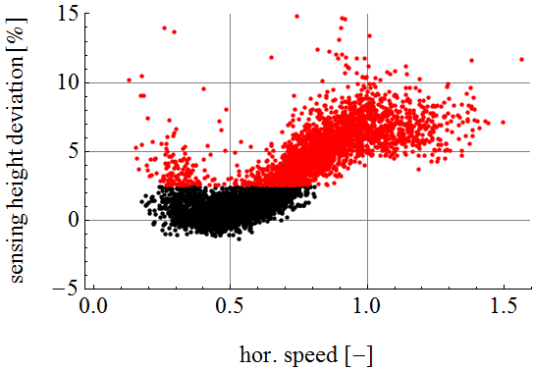

Figure 50 Measurement height (relative to hub height) corresponding to the 10 minute maximum lidar tilt; data within hub height +/- 2.5% (black), data outside the range hub height +/- 2.5% (red)

Acknowledgements

The work described in this report has been carried out under an EUDP funded project (journal no. 64009-0273).

The authors are grateful to Mathieu Bardon and Marc Brodier, from Avent Lidar, Babak Diznabi, from DONG Energy, and the DTU's technicians for the installing and operating the instruments.

Thanks to my close colleagues Mike Courtney and Troels Friis Pedersen for many good discussions.

Finally thanks to Rebeca Rivera (DONG Energy) and Ioannis Antoniou (Siemens Wind Power) for their many good comments to this analysis.

DTU Vindenergi er et institut under Danmarks Tekniske Universitet med en unik integration af forskning, uddannelse, innovation og offentlige/private konsulentopgaver inden for vindenergi. Vores aktiviteter bidrager til nye muligheder og teknologier inden for udnyttelse af vindenergi, både globalt og nationalt. Forskningen har fokus på specifikke tekniske og videnskabelige områder, der er centrale for udvikling, innovation og brug af vindenergi, og som danner grundlaget for højt kvalificerede uddannelser på universitetet.

Vi har mere end 230 ansatte og heraf er ca. 60 ph.d. studerende. Forskningen tager udgangspunkt i 9 forskningsprogrammer, der er organiseret i tre hovedgrupper: vindenergisystemer, vindmølleteknologi og grundlag for vindenergi.

Technical University of Denmark
DTU Vindenergi
Brovej
Building 118
DK-2800 Kgs. Lyngby
Denmark
Telefon 45 25 17 00
info@vindenergi.dtu.dk
www.vindenergi.dtu.dk